DC, AC and noise characterization of InAlN/GaN high electron mobility transistors on SiC substrate

A. GUEN-BOUAZZA*, Z. KOURDI, B. BOUAZZA
University of Tlemcen, Faculty of Technology, Unit of Research, Materials and Renewable Energies P.O. Box 230, 13000, Tlemcen, Algeria

In this paper DC, AC and noise characteristics of an Indium Aluminum Nitride / Gallium Nitride (InAlN/GaN) high-electron-mobility transistor "HEMT" on SiC substrate are investigated. For this device an ultra-thin aluminum oxide Al_2O_3 passivation equal to 25nm is selected for high frequency operation. The device selected for investigation has a gate length of 30nm and a 10nm-thick InAlN barrier layer. Our device exhibit a transconductance gm of 740mS/mm, I_{max} of 590 mA/mm, a cutoff frequency f_T of 300 GHz, a maximum oscillation frequency fmax of 710 GHz., a DIBL of 41.66 mV/V, a dissipated power of 14W/mm and 64% Peak PAE. In this work Noise figure (NF) and low-frequency noise (LFN) are also investigated. Our device performances have been characterized over a wide frequency range.

(Received February 15, 2015; accepted October 28, 2015)

Keywords: InAlN/ GaN, HEMTs, Microwave noise, Min Noise figure, HEMT noise analysis, Silvaco TCAD

1. Introduction

First constructed by Mimura, and al, in 1980 the high-electron mobility transistor (HEMT) is a different form of field effect transistors but similar in structure to the MOSFETs. It exploits the properties of non-Silicon semiconductors. Recently, HEMT has made fast evolution through its characteristics as high power and high frequency device and is nowadays implemented in mobile, military and satellite applications. HEMTs are considered as being the most mature transistors of this new generation and are the most promising high-speed power amplifiers yet seen. The working frequency of HEMT usually varies between 10 to 110 GHz according to their manufacturing material [1-5], knowing that the quality of the material used is the way allowing to achieve optimal device performances [6] . The material optimization of HEMT transistors is difficult and usually focused on increasing the electron's mobility, velocity, and density and on improving its confinement to the channel layer. Gallium Nitride-BASED HEMTs show an enormous potential in high power amplifiers at microwave frequencies. HEMTs become one of the prime candidates for solid-state power amplifiers at microwave frequencies above 30 GHz and this is mainly due to their wide band gap features of high electric breakdown field strength, high electron saturation velocity and high operating temperature. The high power density combined with the comparably high impedance achievable by these devices offers new interesting possibilities for wideband power microwave systems. Additionally, in order to extend GaN HEMTs to millimeter-wave frequency applications, thinner top barriers are required. These thin top barriers allow minimizing short channel effects and also enable higher cutoff frequencies. Unfortunately, AlGaN/GaN 2-D electron gases are subject to surface depletion effects as soon as the top barrier thickness is thinned below 15 nm [7]. This problem has been resolved by using AlN thin top barriers in order to boost channel sheet densities [8]. AlInN was then proposed by Kuzmík as an alternative lattice matched barrier for GaN-based HEMTs at a composition of 83% Al [9]. InAlN/GaN heterostructure considered in our study has the advantage of lattice matching between the $In_{0.17}Al_{0.83}N$ barrier and the GaN channel layer, which could potentially lead to a high quality heterostructure.

Improvement of microwave amplifiers and receivers performances requires knowledge of noise behavior of these amplifiers /receivers designed by HEMT devices [10]. In this work examination of noise contribution of the studied device has been achieved since this study allowed characterizing device performances over wide frequency range. Noise study is essential since it provides information on the lower limits of the signal being processed by a circuit with no considerable deterioration in the signal quality.

2. Noise in (InAlN/GaN) HEMTs

During the past few years, noise performance of field effect transistors has been improved significantly.

Obviously, noise represents an unpredicted random interference. Knowledge of noise phenomena, in active or passive elements, is very important for device modeling in particular and entire circuits design in general. It has considerable impact on circuit performance. It is important to understand noise properties to minimize its effect. The noise performance of field-effect transistors has been a subject of different studies for more than 25 years and

remains to be until now a subject of vigorous research as High Electron Mobility Transistors continue to set records of noise performance.

Generally, in order to quantify the noise performance, the concept of noise figure is used. As an indication, HEMTs are commonly used in different areas due to the fact that they operate at high frequencies with low noise. A minimum noise figure of 0.60 dB at 10 GHz was achieved in AlGaN/GaN HEMT on SiC with a gate length of 0.15µm [11]. An AlGaN/GaN HEMT on a SiC substrate with a gate length of 0.12µm showed a minimum noise figure of 0.98 dB at 18 GHz [12]. There are different noise figure models used for HEMTs. The work by van der Ziel, Fukui, Pucel, and Pospieszalski is the basis for the majority of other investigations and modeling of noise figure. A high-frequency noise model has been proposed by Pospieszalski [13].

Pospieszalski model uses small signal circuit elements that yield closed-form expressions for the noise parameters [12]. This model neglects any correlation between the input voltage noise source and drain current noise source. For HEMT transistors, small-signal equivalent circuit model with the element values of the operating point and all resistive elements used, exhibit a noise contribution that is determined by the physical temperature of the device. Different works reported the excellent agreement of simulated and measured noise parameters with this temperature noise model. In this model, the input voltage noise source is equivalent to the thermal noise of the real part of the input admittance.

The small-signal equivalent circuit model of Pospieszalski shown in Fig. 1 was extended for large signal applications and is used for HEMTs with the adequate noise sources proves to be an adequate representation for HEMTs in a frequency range up at least to 25 GHz.

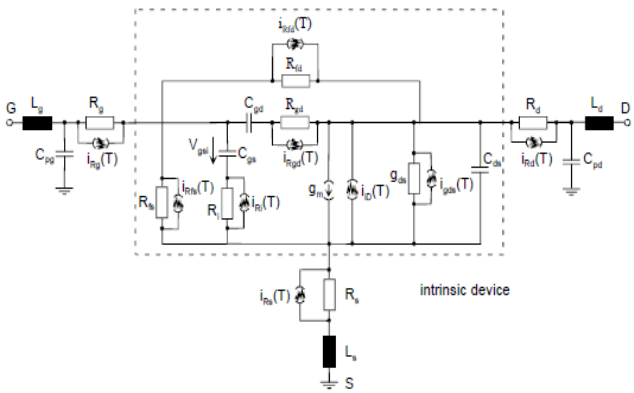

Fig.1. Noise equivalent circuit model of HEMT.

The noise figure usually used for noise investigation is defined as being a measure of the extra noise that the device adds to the signal reaching the load. It is also defined as the noise power delivered to the load, by the noisy source and the noisy device, divided by the noise power that would be delivered to the load if the source was noisy but the device was ideal.

3. Device structure

Fig. 2 shows the InAlN/GaN on 4H-SiC substrate under study, with a cross section of epitaxial layer structure. Our structure contains an AlN buffer layer, a 37nm undoped GaN layer and a 10 nm InAlN layer with a uniform doping density of 1E17 atoms/cm^3 and 83% Al mole fraction. An electron concentration of 1E21/cm^3 is assumed for the source and drain regions. In our design, the peripheral gate oxide Al_2O_3 is different compared to conventional designs.

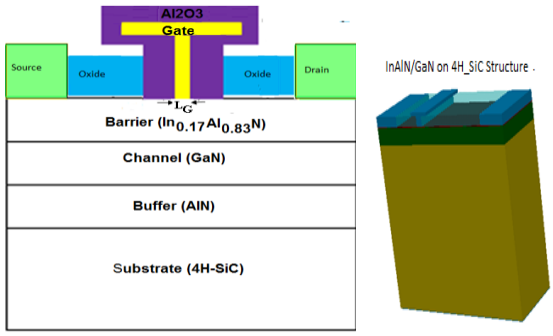

Fig. 2. Device and schematic diagram of the InAlN/GaN HEMT under study.

4. Results and discussion

In this study, two-dimensional simulations have been performed using SILVACO International device simulation software, which proved to be a suitable tool for the hetero- structure devices analysis. ATLAS program performed the general functions while BLAZE, GIGA, and C-INTERPRETER performed specialized functions required for III-V heterojunction devices, thermal calculations, and user defined equations, respectively. In order to control and modify the models used DECKBUILD, DEVEDIT and TONYPLOT have been employed.

A. DC performances

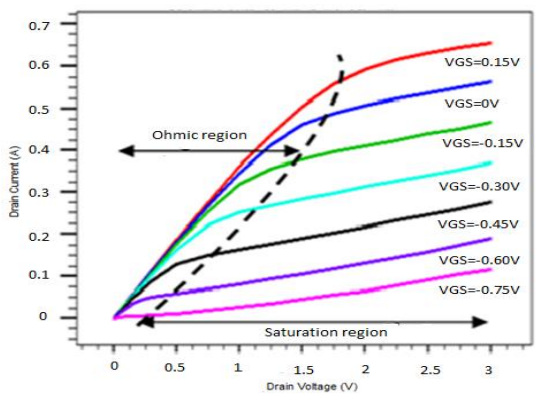

Fig. 3. Output characteristics of the InAlN/GaN HEMT simulated

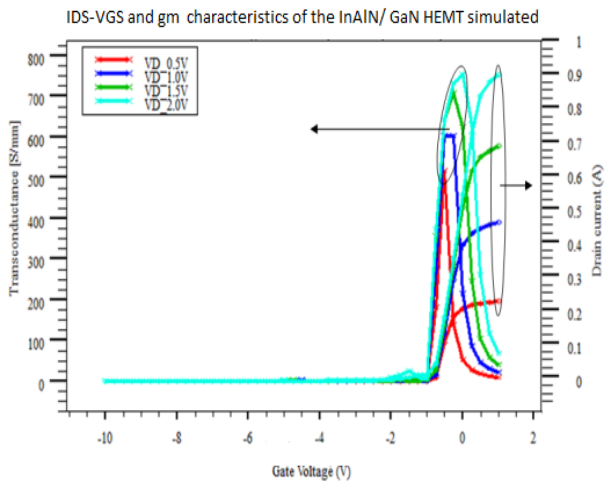

Fig. 4. Transconductance and transfer characteristics of the studied InAlN/GaN HEMT.

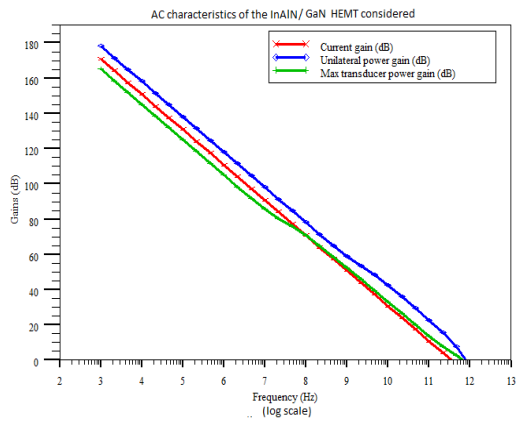

Fig. 5. Simulated current gain (H_{21}), unilateral power gain (U) and max transducer power gain (MTG) versus frequency for the InAlN/GaN HEMT. The bias condition are V_{DS}=2V and V_{GS}=0V.

Fig. 3 shows the I_{DS}–V_{DS} characteristics of our HEMT simulated over V_{DS} = 0−3 V with V_{GS} = 0.15 to –0.75 V.

One of the most important advantages of the InAlN/GaN heterostructure is the elevated interfacial sheet charge density that should allow a very high current level density. Our AlInN/GaN HEMTs feature a maximum current density of 590 mA/mm at VGS=0V as shown in Fig. 3

The transconductance g_m is an important parameter that has to be optimized for microwave performance of HEMT transistors. In Fig. 4, the transconductance is plotted as function of V_{GS}. This figure exhibits gm- V_{GS} in its left side and I_{DS}-V_{GS} characteristics in its right side.

The transfer characteristic is used to determine the threshold voltage, V_{TH}, and the transconductance g_m. Our device exhibited excellent pinch-off of -1.23V, a low knee voltage, and a high peak transconductance of 740 mS/mm at V_{DS}=2V. In fact, HEMT devices are distinguished from all other field effect transistors by their high transconductance and this is the case of our device. The gate characteristic, also allows evaluating the gate Schottky contact quality. Depending on the shape of this characteristic, and the magnitudes of the gate current, it is possible to extract the barrier height of the gate contact and to evaluate the leakage current of the device. For RF applications, it is very interesting to obtain the lowest gate current, because this current tends to increase the noise component in this frequency range.

B. AC performances

The frequency device performance is studied by small-signal AC analysis. Fig. 5 shows simulation results we obtained allowing determining our device current gain H_{21}, its maximum transducer power gain and its unilateral power gain.

The maximum current gain H_{21} obtained for our HEMT is equal to 180 dB, the maximum transducer power gain is equal to 120 dB and the maximum stable power gain is equal to 90 dB. Our simulation results also indicate that the structure has a cutoff frequency f_T of 300 GHz and Maximum frequency fmax of 710 GHz. The simulation results we obtain meet the expectations of a superior microwave performance for AlInN/GaN HEMTs in comparison to results of more mature AlGaN/GaN HEMTs.

C. Noise characteristics

The noise performance of HEMT devices is strongly dependent on the spacer thickness: indeed, the thin spacer layer separating electrons from their donors allows reducing the scattering of electrons by the positively charged donors. This is achieved by introducing a thin spacer layer of undoped AlN between the InAlN donor layer and the GaN channel layer in order to separate the negatively charged 2-DEG from the ionized dopant atoms.

The main benefits of InAlN studied over AlGaN structure include lattice matching with GaN with Indium content of 17% and high spontaneous polarization, allowing to create high charge carrier densities in 2DEG electron gas that is formed at the InAlN/GaN interfaces. These properties allow improving electrostatic control of the device current that flow through the device.

In our study a thin spacer layer of approximately 1nm thickness have been used for low-noise and power devices by reason of the reduced parasitic source resistance and the increased of current density and transconductance allowing to reduce the alloy related interface roughness and to improve significantly the electron mobility.

In order to perform noise analysis with SILVACO-TCAD, Noise module combined with Blaze allows analysis of the small-signal noise generated within semiconductor devices. The Noise simulation module in atlas employs the impedance field method derived by Shockley and.al [14]. It provides accurate characterization of all small-signal noise sources and allows to extract all

figures of merit that are essential for the optimization of circuits' design [14].

Fig. 6 shows frequency dependences of the spectral noise density.

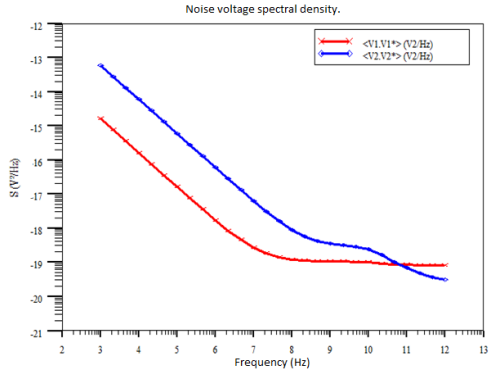

Fig. 6. Noise voltage spectral density of our simulated device at V_{DS}=2V.

As shown in Fig. 6, the noise spectra display typical 1/f noise dependence. It is important to identify flicker noise and to know its value, since this type of noise is the limiting figure for all kinds of HEMT's. Low frequency noise in HEMT structures is important since it becomes a significant limitation of the device performances.

Although discovered very early and nearly everywhere, the source of flicker noise is still not clear. Nowadays, there are several theories which are established by diverse groups for diverse devices and even for the same devices but considered in different operation regions. The two important flicker noise models are McWhorther's (trapping-detrapping) [15] and Hooge's (mobility fluctuation) models [16]. However, flicker noise is always associated with the flow of direct current flowing through the device. 1/f noise is the low frequency noise that affects device performances and that can be ignored at very high frequencies.

Fig. 7 displays drain bias dependence of low frequency noise at room temperature. We can observe that flicker noise dominates at low frequency. It is important to identify flicker noise, since this low frequency noise is the limiting figure for all kinds of HEMT devices. Noise spectral density varies with frequency variation. Our device has a low output noise.

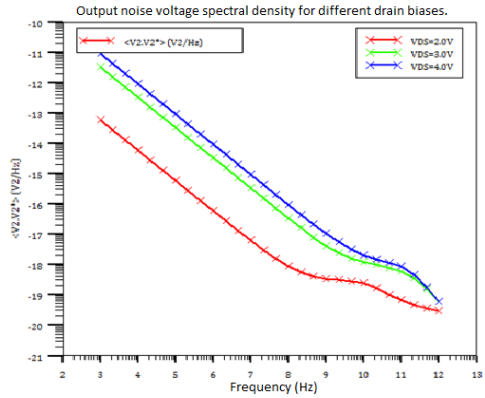

Fig. 7. Drain bias dependence of low frequency noise.

Our results highlights clearly that the low frequency noise is affected by the bias voltage V_{DS}. The biasing voltage increasing generates a net increase in noise spectral density. Our simulation results allow to observe that noise spectral density at V_{DS}=4V is greater than noise spectral density at V_{DS}=2V.

We can than conclude that with the drain bias increasing, the noise power density of high frequency part increases. That means that there are more short time constant trapping and detrapping taking place at a high V_{DS} bias or at high electric field between the drain and the gate. We can add that in these structures in two-dimensional electron gas, it is assumed that flicker noise dominates at low frequency. Indeed, the spectral density of voltage noise decreases when V_{DS} decreases implying a low bias voltage leads to a lower noise level. The effect of bias voltage on the intensity of the noise is obvious. The linearity shown in our results reflects the fact that the noise comes mainly from the channel.

It is worth noting that at high frequencies the principal source of noise added by the transistor is related to power dissipation in the resistances of the device.

The extracted noise parameters allowing performing noise analysis are noise figure, noise conductance, and noise impedance Zo.

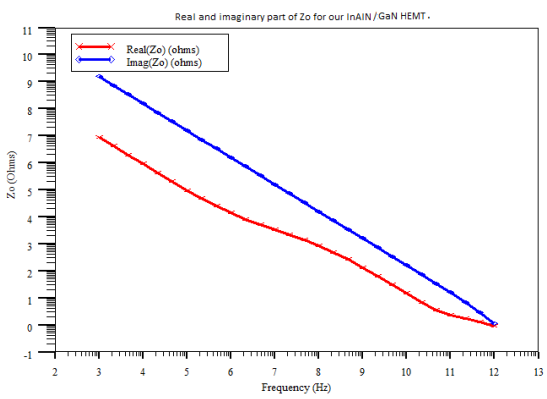

Fig. 8. Real and imaginary part of Z_0 versus frequency

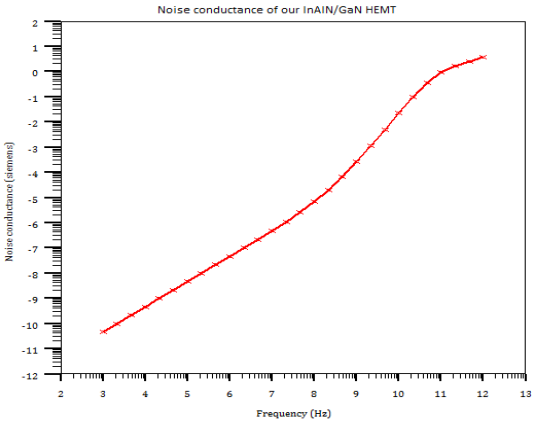

Fig. 9. Variation of noise conductance with frequency. The drain bias voltage is 2V

Noise figure is the mostly used parameter allowing qualifying the noise performance of circuits. It is used as a measure of noise performance of a noisy 2-port network. It is defined as the Signal/Noise ratio at the input port divided by Signal/Noise ratio at the output port. NF is generally affected by the source input impedance at the input port of the network and the noise sources in 2-port network itself.

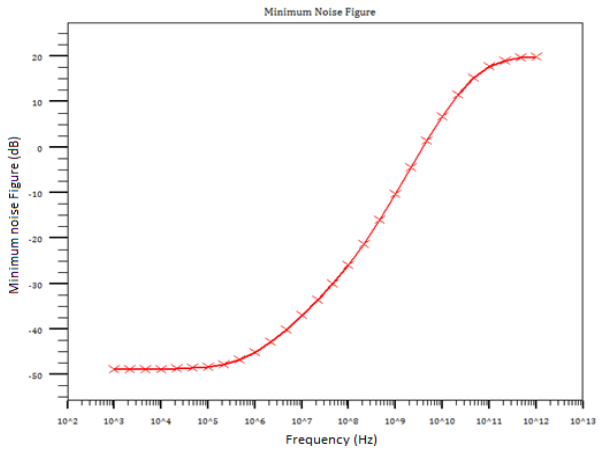

Fig. 10. Minimum noise figure versus frequency. Drain bias voltage is equal to 2V.

Fig. 9 and Fig.10 show respectively the simulated conductance noise and the simulated minimum noise figure for the extrinsic device we obtained using Atlas simulation Silvaco and C-interpreter that allowing to define noise models. As shown from our results, noise figure increases with frequency increasing. Our simulated model has noise figure of 0.0 dB at frequency equal to 50GHZ and 20dB at frequency equal to 1THz.

The noise figures of HEMTs can be further improved by reducing additional noise contributions from parasitic, especially at high frequency. It is also important to notice that noise has a relationship with f_T and f_{max} such that improvements in one of these quantities mean an improvement in the others. To end, there is the matter of device bias. As the transistor DC bias changed, noise parameters change correspondingly.

In order to observe NFmin variation with V_{DS} variation, NFmin is simulated versus frequency at a fixed bias V_{GS}. Simulated results we obtained are depicted in Fig.10.

Transistors in LNA are biased at low currents and voltages for maximum NF performance and to reduce power consumption. So, it is amount of importance to know how the noise parameters change with device biases.

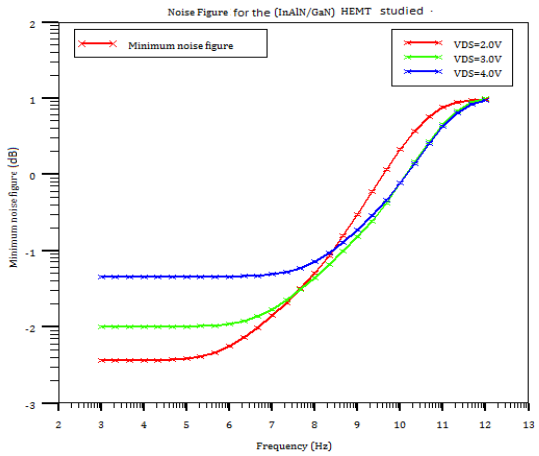

Fig. 11. Drain bias dependence of minimum noise figure NF.

It is noticeable that there is no significant increase in NFmin in high frequency part where NFmin is essentially constant with V_{DS} increasing and this is mainly due to the fact that V_{DS} increasing isn't so significant. For higher V_{DS}, NFmin increases and this is due to some factors that are g_m reduction, drain current increasing , and dissipated power increasing.

5. Conclusion

In summary, this work assesses performances of a 30nm gate length InAlN / GaN HEMTs on 4H-SiC substrate where DC and AC analysis have been performed using SILVACO-TCAD software. In this work, device noise contribution has also been investigated. The studied device shows well-behaved characteristics. Promising characteristics of minimum noise figure have been obtained. Minimum noise figure of our device can be further reduced by reducing the noise contributions from parasitic. At the end of this study, we can say that our simulation results confirm the feasibility of using HEMTs with InAlN/GaN in high power amplifiers. Our results also demonstrate the viability of InAlN/GaN HEMTs for robust low-noise amplifiers. We can add that InAlN/GaN HEMT devices exhibit promising microwave noise properties that are comparable to those of AlGaAs/GaAs and AlGaN/GaN HEMTs.

References

[1] T. Mimura, IEEE Trans. On Micr. Theory and Tech., **50**(3), 780 (2002).
[2] G. Crupi, D. M. P. Schreurs, A. Caddemi, Int. Journal of RF And Micr. Comp.-Aided Eng., 417 (2008).
[3] L. T. Wurtz, IEEE Transactions on Instrumentation and Measurement, **43**(4), 655 (1994).
[4] D. S. Chalermwisutkul, PhD. Thesis, Aachen University, Germany, 25 (2007).
[5] G. Crupi, D. Xiao, D. Schreurs, E. Limiti, A. Caddemi, W. De Raedt, M. Germain, IEEE Trans Microwave Theory Tech., **54**, 3616 v3622, 2006.
[6] J. Javier Bautista «,HEMT Low-Noise Amplifiers ».
[7] M. Higashiwaki, T. Mimura, T. Matsui, Proc. SPIE, 2008, **6894**, no. 1, Proc. SPIE. **68941**. doi: 10.1117/12.791601. http://dx.doi.org/10.1117/12.791601.
[8] Y. Cao, D. Jena, Appl. Phys. Lett., **90**(18), 182 112 (2007).
[9] J. Kuzmík, IEEE Electron Device Lett., **22**(11), 510 (2001).
[10] A. Balandin, S. Cai, R. Li, K. L. Wang, V. Ramgopal Rao, C. R. Viswanathan, IEEE Electron Device Letters, **19**(12), (1998).
[11] C. Lee, H. Wang, J. Yang, L. Witkowski, M. Muir, M. A. Khan, P. Saunier, Electron. Lett., **38**, 924 (2003).
[12] N. X. Nguyen, M. Micovic, W. S. Wong, P. Hashimoto, J. Janke, D. Harvey, C. Nguyen, Electron. Lett., **36**, 469 (2000).
[13] M. W. Pospieszalski, IEEE Trans. Microwave Theory and Techn., **37**(9), 1340 (1989).
[14] http://www.silvaco.com/products/vwf/atlas/noise/noise_06.pdf.
[15] A. L. McWhorter, R. H. Kinston, Ed. Philadel-phia: Univ. of Pennsylvania Press, 207 (1956).
[16] F. N. Hooge, T. G. M. Kleinpenning, L. K. J. Vandamme, Rep. Prog. Phys, **44**(5), 479 (1981).

*Corresponding author: guenahlam@yahoo.fr